Histochem Cell Biol (2008) 130:177–184
DOI 10.1007/s00418-008-0415-x

ORIGINAL PAPER

Ultrastructural localization and chemical binding of silver ions in human organotypic skin cultures

Søren Kristiansen · Peter Ifversen · Gorm Danscher

Accepted: 10 March 2008 / Published online: 5 April 2008

Abstract Organotypic cultures of human breast skin incubated with silver bandage or treated with silver sulfadiazine accumulated silver in epithelial cells and in macrophages, fibroblasts and collagen fibrils and fibres of underlying connective tissue. Ultrastructurally, the accumulated silver was found in lysosome-like vesicles of the different cells and evenly spread along collagen structures. Apoptotic nuclei were present but few. Autometallographic amplification of 2D-PAGE gels revealed that glutathione S-transferase and glutathion detoxify silver ions in the epidermal cell by binding them in silver–sulphur nanocrystals. Thus, the cytotoxic effect of silver ions seems to be muted by silver ions by being: (1) taken up by undamaged cells, neutralised by glutathione (GSH) and accumulated in lysosomal vesicles, (2) bound extracellularly to SH-groups of the collagen fibres.

Keywords Silver · Wound healing · Glutathione S-transferase · Autometallography · Multiple resistance proteins · Gluthatione

Introduction

Silver has been used in a multitude of commercially available wound dressings as an antiseptic agent. These products are all based on chemically bound silver ions as silver in its metallic form has been considered to process little or no oligodynamic effect, i.e., antimicrobial properties (Bicanova and Thinschmidt 1985).

Silver ions are biologically active and believed to react chemically mainly with SH-groups present, e.g., in cystein. Due to the readiness by which silver ions interact with proteins the acute and long-term cytotoxicity of silver has been discussed rather intensively (Burd et al. 2007; Lansdown 2007; Lansdown 2006; Brett 2006; Hollinger 1996). It has been found, e.g., that long termed exposure to silver salts causes depositions of silver sulphide accumulations (argyria) in almost all organs. This intensive accumulation seems not to be a life threatening condition although unwanted for obvious cosmetic reasons (Aaseth et al. 1981; Danscher 1981). Since silver ions bind so avidly to sulphide, it has been suggested that silver ions used to treat infections bind to the cystein-rich metallothionein in the exposed tissue (Lansdown 2002; Lansdown 2007; Lansdown 2006). Metallothioneins have proved to bind silver and other toxic metal ions in vitro (Scheuhammer and Cherian 1986) and to be significantly up regulated in wounds exposed to zinc, copper and cadmium (Lansdown et al. 2001; Lansdown et al. 1999).

In a recent review study on the fate and cytotoxicity of silver applied to wounds, the presence of silver in the tissues was analysed in histological sections as what the authors call "natural precipitations" and quantified by atomic absorption (Lansdown 2007; Lansdown et al. 2005). The histochemical "precipitation" approach can only be used after extensive exposure to silver and the atomic absorption approach involves a complete destruction of the histology. The histochemical technique autometallography (AMG), however, enables amplification of tiny amounts of the metal, i.e., down to a few silver atoms (Danscher 1981; Danscher and Stoltenberg 2006). The high sensitivity of

S. Kristiansen (✉) · P. Ifversen
Wound & Skin Care, Cell Group, Coloplast,
Bakkegaardsvej 406A, 3050 Humlebæk, Denmark
e-mail: dkskn@coloplast.com

G. Danscher
Department of Neurobiology, Institute of Anatomy,
University of Aarhus, 8000 Aarhus C, Denmark

AMG allows tracing of the fate of silver ions in organisms that have been exposed to even very low levels of silver. In the present study we have (1) traced the exact localization of silver at both LM and EM magnifications, (2) demonstrated gluthatione S-transferase as a silver-binding protein.

Gluthatione S-transferase is expressed in all cell types and involved in detoxification of xenobiotics and metals by conjugation with glutathione (GSH) (Deeley et al. 2006; Ralat and Colman 2004; Cole and Deeley 2006).

Materials and methods

Preparation of human in vitro wounds

Pieces of human skin were obtained from routine breast plastic reduction surgery as approved by the local ethic committee. The wounds were made in the skin specimens by a modification of the protocol as previously described (Jansson et al. 1996). In brief, the subcutaneous fat was mechanically removed from the skin under sterile conditions. On the epidermal site, a wound was made with a 4 mm punch biopsy instrument (Produkte für die Medizin AG, Cologne, Germany). Each skin specimen provided with one artificial wound was transferred to a six well plate (Costar Cambridge, MA). The air-lifted organotypic preparation was incubated in Dulbeccos Modified Eagles Medium (DMEM, BioWhittaker Cambrex) supplemented with antibiotics (100 U/ml pencillin, 100 µg/ml streptomycin and 25 µg/ml amphotericin B), 10% (vol/vol) foetal bovine serum (FBS, BioWhittaker, Cambrex) and hydrocortisone (0.4 µg/ml). The experimental organotypic preparations were covered by a silver containing foam dressing (Contreet, Coloplast, Humlebæk, Denmark) soaked in DMEM, or the preparation was incubated in DMEM supplemented with 20.0 µg/ml silver sulfadiazine. Controls were only incubated in DMEM. The control and silver stimulated skin specimen were then incubated for 3 days in a humidified CO_2 incubator at 37°C.

Autometallographic tracing of silver–sulphur nanocrystals

The organotypic skin cultures were immersion fixed in buffered formalin or glutaraldehyde and embedded in either paraffin or Epon. The silver–sulphur nanoparticles resulting from metabolism of the invading silver ions were then silver enhanced in tissue sections from the two sources by being subjected to an AMG developer.

In short, the section containing slides were placed in jars and covered with the AMG developer. The developer consisted of a 60 ml gum arabic solution and 10 ml sodium citrate buffer (25.5 g of citric acid $1H_2O$ + 23.5 g sodium citrate $2H_2O$ to 100 ml distilled water), 15 ml reductor (0.85 g of hydroquinone dissolved in 15 ml distilled water at 40°C), and a 15 ml solution containing silver ions (0.12 g silver lactate in 15 ml distilled water at 40°C) added immediately before use while thoroughly stirring the AMG solution (Stoltenberg and Danscher 2000). After being developed for 60 min in a water bath at 26°C covered with a light tight hood the developer was replaced with 5% sodium thiosulfate that stopped the development. After 10 min the sections were rinsed several times in distilled water and mounted.

Paraffin sections

The slices were embedded in paraffin and 5-µm-thick sections were cut, placed on glass slides and AMG developed. After a careful rinse they were counterstained with toluidine blue and mounted in DEPEX.

Epon sections

The areas to be analyzed in the electron microscope were dissected from vibratome slices that had been AMG developed. Some of these small blocks of tissue were placed in a vial where they were fixed in 0.1% osmium tetroxide for 30 min. Fixed and unfixed blocks were then, after proper rinsing in distilled water, embedded in Epon. From the Epon blocks 3-µm-thick sections were cut, counterstained with toluidine blue and analyzed in the light microscope. Sections to be analyzed ultrastructurally were then embedded on top of a blank Epon block, and after proper trimming ultra thin sections were cut and stained secundum artem (Danscher and Stoltenberg 2006; Danscher 1981).

Dose-response of silver sulfadiazine

Epidermal human cell cultures (HaCat) were incubated for 3, 24 or 48 h with DMEM containing 10% FCS alone (control) or supplemented with 1.25, 2.50, 5.00, 10.00 or 20.00 µg/ml of silver sulfadiazine. After the designated time-point the epidermal cells were extensively washed with PBS and thereafter stained with propidium iodid and SYTO 9 (Molecular Probes). The intensity of the fluorescence signals was determined and related to the signal from the control preparation incubated for 3 h.

Detection of silver-binding proteins by 2D-PAGE and AMG

Control- and silver-stimulated (2 days with 5.0 µg/ml silver sulfadiazine) cell cultures were collected after centrifugation. A protein lysate was made with PBS containing 0.5% (vol/vol) NP-40. The lysate was acetone precipitated, and the protein pellet was dissolved in 7 M urea, 4% CHAPS, 3% Pharmalyte 3–10 (Amersham Biosciences), 2% dithiothretiol and added bromphenol blue as a visual tracer. The

1-dimensional strip (pH 3–10, length 13 cm, Amersham Biosciences) was incubated overnight with the protein sample. Next day the strip was isoelectrically focused on a Multiphor II apparatus (Amersham Biosciences) equipped with a cooling plate cooled to 16°C. The power supply (EPS 3501 XL) was programmed with the running conditions as suggested by the supplier (Amersham BioSciences). After focusing, the strip was incubated for 10 min in equilibration buffer (50 mmol/l tris pH 6.5, 6 mol/l urea, 30% glycerol, 2% SDS) added 4.0 mg/ml dithiothretiol, then again in equilibration buffer supplemented with 45.0 mg/ml iodo acetoamide. The isoelectrically focused proteins in the strip were then separated in the second dimension (Hoefer SE 60) on a 10% or 15% SDS polyacrylamide gel. Proteins in the gel were visualized by silver staining (Shevchenko et al. 2004), or the gel was washed extensively in water before developed by AMG. Protein spots were excised from the AMG developed gel with a clean razor blade and the in-gel proteins were degraded by trypsin (Shevchenko et al. 2004). Peptide fragments were analyzed by nanoESI MS/MS on a Q-TOF mass-spectrometer. The resulting amino acid profile was compared to known peptides by database searching in the NCBInr by Mascot, MatrixScience (Institute of Technology, Kolding, Denmark).

Purification and activity of the gluthatione S-transferase enzyme

A post-nuclear supernatant was made by dissolving cell cultures with PBS containing 1% triton X-100. The supernatant was cleared through a 20 µm filter and purified on GSH-agarose column (Sigma–Aldrich). The column was extensively washed with PBS before eluted with PBS containing 10 mmol/l GSH. The eluted sample was dialysed in PBS in order to get rid of excess GSH. The dialysed sample was stored at −20°C. The purity of the sample was checked by separating the protein by SDS-PAGE followed by silver staining. The gluthatione S-transferase activity was measured by using CDNB (chlorodinitrobenzene) as a substrate (Ishikawa et al. 1994; Li et al. 1996). In brief, 0.2 ml PBS containing 1 mmol/l CDNB was added different concentrations of silver lactate and GSH before the background absorption was measured at 340 nm. Then 5 µl of the purified gluthatione S-transferase sample was added and the activity was measured at different time-points.

Formation of GS-silver complexes was evaluated by anion-exchange chromatography and atomic absorption (Ishikawa and Ali-Osman 1993). In brief, silver lactate and GSH were dissolved in water at a concentration of 40 mmol/l. NaOH added drop by drop cleared the cloudiness of the solution. The silver lactate/GSH solution was applied to a QAE-Sephadex anion-exchange column (bed volume 1 ml) equilibrated with 10.0 mmol/l tris pH 7.5. The column was washed extensively with the equilibration buffer before the bound GS-silver complex was eluted with 0.2 M HNO_3. Atomic absorption was used to measure the concentration of silver bound to the column material.

Reverse transcription and real time PCR

DNA-free RNA was isolated with the Absolutely RNA® kit (Stratagene). RNA was reverse transcribed with an M-MLV enzyme (USB Corporation, Cleveland, OH) and oligo(d)$T_{12–18}$ primers. Real time PCR was performed on a LightCycler 1.2 system using the MasterPlus SYBR green kit (Roche). Samples not subjected to the RT reaction were used as negative controls. Lack of unspecific primer–dimer formation of the cDNA was checked by analysis of melting curves, and the length of the resulting cDNA was checked by separation on a TBE agarose gel. The primers used for GSH synthase, MRP2 and β-actin mRNA were aactaga agtgcagttgacat (sense) and gctccaaggaaagattaactc (antisense), tcctcattcctggacagtccgg (sense) and gagtcttctgtgagtacaagggcc (antisense), and gacatccgcaaagacctgtac (sense) and tgcc agggcagtgatctcc (antisense), respectively.

Statistics

One tailed t test analysis was carried out on the two data samples with equal variance. The significance value was set at $p < 0.05$. Data are expressed as mean ± standard error.

Results

AMG tracing of silver released from the dressing

The typical morphological structures of a closing wound with lateral migrating keratinocytes were seen in the organotypic skin cultures. In the epidermis silver was found in the keratinocytes located in vesicular organelles (Fig. 1a). The untreated controls were blank (Fig. 1b). The dermal papillae contained an overwhelming amount of silver-loaded macrophages, and fibroblasts in the intact tissue adjacent to the wound and the rather delicate collagen fibres were dotted with AMG grains. Silver also accumulated in hair follicles (Fig. 1c) and sweat glands located in the undamaged connective tissue around the wound. At the bottom of the wound, deep in the main dermis, the collagen fibres were also heavily dotted with silver, and most of the fibroblasts and macrophages were loaded. The majority of the invading silver ions accumulated a few millimetres into the wound walls and in the layer of proliferating and lateral migrating keratinocytes at the edges of the wound (Fig. 1d). The AMG enhanced silver–sulphur nanoparticles were

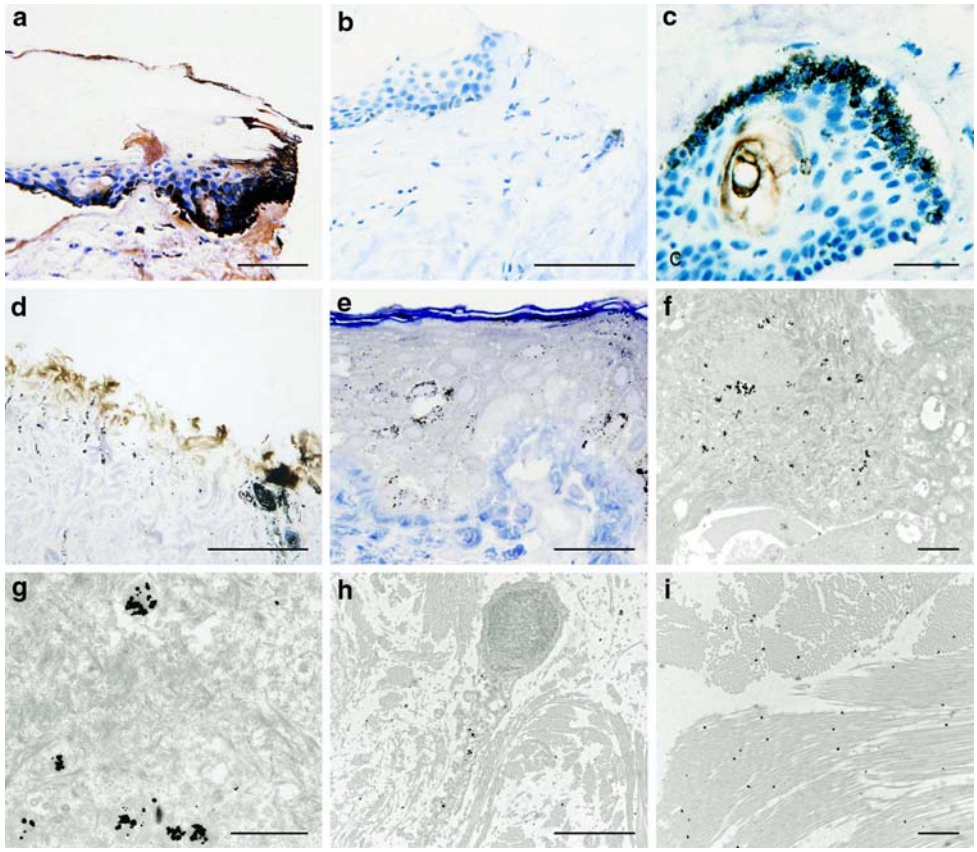

Fig. 1 Wounds were induced in breast skin and allowed to heal for 3 days with or without silver dressing. Cryostat, paraffin and Epon sections were AMG developed and analysed by light microscopy (**a**–**e**) or electron microscopy (**f**–**i**). **a** Light microscopy at the edge of the artificial wound with laterally migrating keratinocytes heavily loaded with AMG enhanced silver nanoparticles in the perinuclear region. Cryostat section counterstained with toluidine blue. *Scale bar* 100 μm. **b** AMG developed control section showing the wound edge. Note the total lack of AMG staining. Cryostat section counterstained with toluidine blue. *Scale bar* 150 μm. **c** Micrograph of paraffin section AMG enhanced and counterstained with toluidine blue. The most *right part* of the picture is close to the wound edge. Note the strong staining of the external root sheath cells closest to the wound. *Scale bar* 50 μm. **d** Micrograph of the wound bed showing AMG enhanced silver accumulations. Note the AMG staining of the collagen fibers of the wound bed. Paraffine section counterstained with toluidine blue. *Scale bar* 500 μm. **e** Shows silver loaded keratinocytes located further away from the wound edge. Three micron thick Epon embedded section counterstained with toluidine blue. *Scale bar* 50 μm. **f** Electron micrograph of keratinocyte showing that silver accumulates in lysosome-like organelles. *Scale bar* 2 μm. **g** Electromicrography at a higher magnification revealing the silver loaded lysosomes in the cytoplasm of a keratinocyte. *Scale bar* 1 μm. **h** Fibroblast containing silver in lysosome-like organelles. Note the punctuated AMG grains associated to collagen fibers. *Scale bar* 4 μm. **i** Collagen fibers dotted with AMG enhanced silver deposits. The picture was taken somewhat away from the wound walls where the concentration of silver ions is low. The intensity gradient of silver from the wound edge and to tissue totally free of silver is very steep for silver bound to collagen as compared to silver containing cells. *Scale bar* 2 μm

always found in lysosome-like vesicles (Fig. 1f-h). As shown in Fig. 1i, silver did not only accumulate in cells and on collagen fibres in the wound bed, but could be traced deep into the underlying subcutaneous layers.

Skin biopsies subjected to 20.0 μg/ml silver sulfadiazine dissolved in the medium accumulated silver intra- and extracellularly in a way identical to that observed in preparations exposed to the silver releasing dressing (data not shown).

Stimulation protocol for the epidermal cell cultures

In order to have maximal stimulation of any putative detoxifying mechanism we did time-course dependent measurements of the number of living epidermal cells after incubation with increasing amounts of silver sulfadiazine. As shown in Fig. 2, the number of living cells did not decline significantly after 3, 24 or 48 h if the concentrations were kept below 5 μg/ml of silver sulfadiazine. At 5 μg/ml, the number of living cells declined significantly after 24 h when compared to the controls, but the decline stopped at longer exposure times, i.e., the cells recovered after 48 h. When the silver sulfadiazine concentrations were increased to 10 and 20 μg/ml the epidermal cells did not recover after 48 h and there was a time-course dependent reduction in the number of living cells. In conclusion, the epithelial cell cultures were more sensitive to silver ions than the organotypic skin cultures.

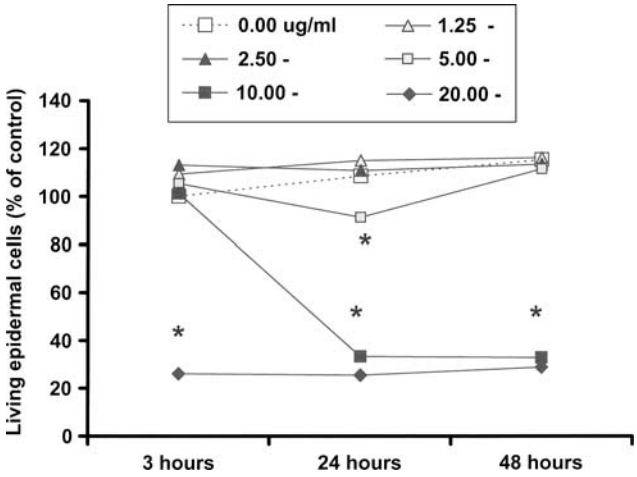

Fig. 2 Epidermal cell cultures were incubated for 3, 24 or 48 h without (control) or with increasing concentrations of silver sulfadiazine, as indicated. The number of living epidermal cells was determined by staining with fluorescence dyes and expressed relative to control value after 3 h

Isolation of silver binding proteins

In order to determine the metal binding proteins responsible for handling the silver ions, we isolated proteins obtained from lysates made from control and silver-stimulated (5.0 µg/ml sulfadiazine for 48 h) epidermal cell culture preparations. The proteins were isoelectrically focused from pH 3–10 and separated by SDS-PAGE on a 10 and 15% gel. The gel was then AMG developed in order to enhance possible silver bound to one or more protein bands. The gels from the controls were completely blank (data not shown), but on the 10% gel from the silver stimulated preparations a band of AMG enhanced silver was observed (Fig. 3). The AMG developed silver spot was excised and analysed by NanoESI maldi-TOF MS/MS and found to be glutathione S-transferase (Ralat and Colman 2004; Terrier et al. 1990; Whalen et al. 1996).

Fig. 3 A protein lysate was made from an epidermal cell culture incubated for 2 days without or with 5.0 µg/ml silver sulfadiazine. The lysate proteins were separated by 2D-polyacrylamide gel electrophoresis and the gel was AMG developed. The *arrow* shows one representative of AMG induced development of a silver binding protein

Since glutathione S-transferase uses GSH as a co-factor to conjugate xenobiotics and metals, we analysed whether GSH binds silver ions. By combining anion-exchange and atom absorption, we found that the positive silver ions alone did not—as expected—bind to the anion-exchange column. But if silver ions and GSH were pre-mixed almost 95% of the silver could be recovered from the anion-exchange column.

To study whether silver interferes with the gluthatione S-transferase activity we applied CDNB as a gluthatione S-transferase substrate and used different concentrations of silver in combination with a low (250 µmol/l) or high (1250 µmol/l) concentration of GSH. As shown in Fig. 4, silver inhibited the gluthatione S-transferase mediated conjugation of CDNB in the presence of the low GSH concentration. The dose-response inhibition of silver was equimolar (approximately 250 µmol/l) with the low GSH concentration, showing that when all GSH was bound by silver the GST enzyme activity was totally blocked. At high GSH concentration the inhibitory effect of silver ions fainted.

Expression of mRNA coding for GSH synthase in keratinocytes

The expression of mRNA coding for GSH synthase in keratinocytes exposed to 5.0 µg/ml silver to 3, 24 or 48 h shows a substantial increase in the expression of GSH synthase in a time-dependent fashion (Fig. 5).

Having shown that silver induces an increase in the GSH synthase activity, binds to GSH and accumulates in lysosome-like organelles, we analysed the expression of mRNA encoding for different multiple resistance pumps (MRP) known to be capable of transporting GSH complexed with metals. We found that when the epidermal cell culture was incubated with 5.0 µg/ml of silver sulfadiazine, silver induced a time-course dependent increase in the expression of the MRP2 isoform (Fig. 6).

Discussion

Despite the evident acute in vitro cytotoxicity of silver ions (Hollinger 1996; Burd et al 2007; Lansdown and Williams 2004; Brett 2006) wound healing in patients and animals treated with silver dressings is a well-known fact (Lansdown et al. 1997; Jorgensen et al. 2005). Thus accumulation of silver in the keratinocytes as shown in the present study does not seem to restrain the closure of the wound, undoubtly because of the presence of detoxification mechanisms.

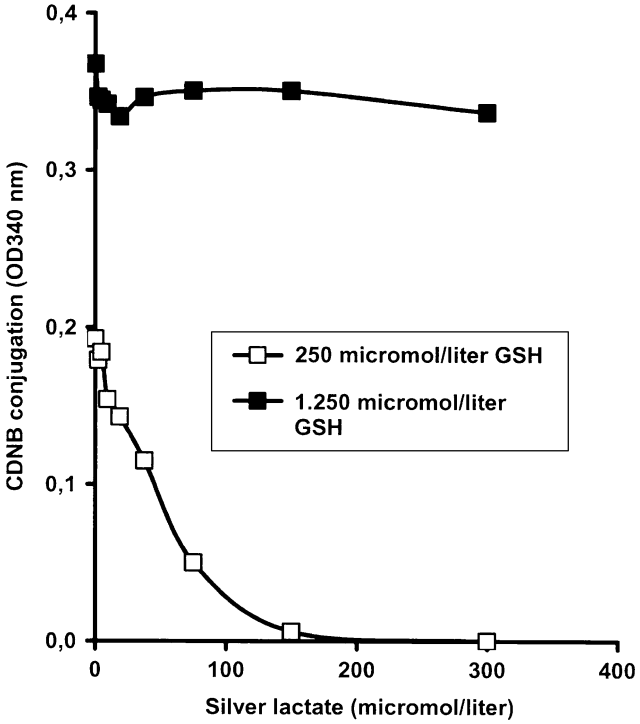

Fig. 4 GST enzymatic activity was measured by conjugation of CDNB with GSH. The final GSH concentration was 250 or 1250 µmol/l, and the silver concentration varied as shown on the *X*-axis. Silver inhibited the GST activity when GSH was kept at 250 µmol/l and 100% inhibition was found at approximately 250 µmol/l of silver lactate

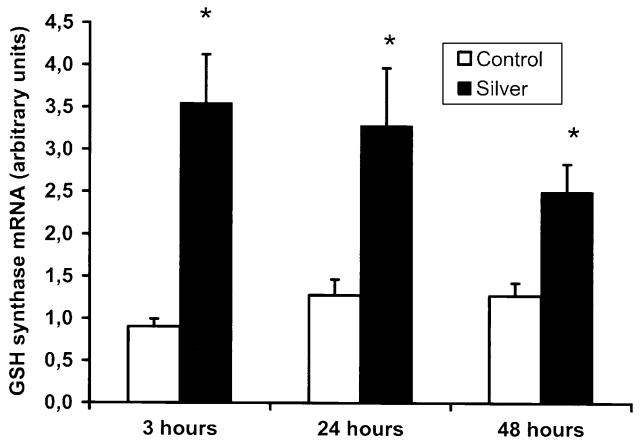

Fig. 5 The expression of mRNA encoding for GSH synthase was measured in epidermal cell cultures exposed to 5.00 µg/ml of silver sulfadiazine for 3, 24 and 48 h. The mRNA concentration was measured by real time PCR and adjusted to the concentration of β–actin. * $p < 0.05$, $n = 6$

A common route of detoxification includes an increased production of metal binding proteins followed by degradation of the silver loaded metal binding proteins in vesicles. Silver ions are known to be accumulated as non-toxic deposits of silver–sulphur nanoparticles in lysosomes. (Danscher 1981; Danscher and Stoltenberg 2006; Rungby

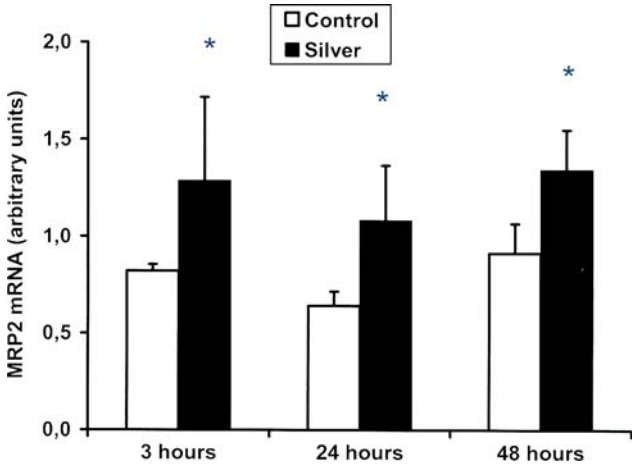

Fig. 6 The expression of mRNA encoding for MRP2 was measured in the epidermal cell culture exposed to 5.00 µg/ml of silver sulfadiazine for 3, 24 and 48 h. The mRNA concentration was measured by real time PCR and adjusted for the concentration of β–actin. * $p < 0.05$, $n = 6$

and Danscher 1984). In the present experiment we observed that silver ions accumulate in lysosome-like organelles of a wide variety of cells in the human organotypic cell cultures. Extracellularly, the AMG enhanced nanoparticles were spotted in reticular fibres in the basement membrane and in differently sized collagen fibres. Thus, migration of cells close to the wound and the differentiation profiles of the healing tissue does not seem to be influenced by the silver exposure in the timetable that we have studied.

By combining 2D-PAGE and AMG analysis we were able to identify a protein that was loaded with silver. The protein was found to be gluthatione S-transferase. Gluthatione S-transferase is known to conjugate toxic xenobiotics and metals with GSH (Cole and Deeley 2006). GSH is at the same time an antioxidant protecting cells from free radicals (Almar and Dierickx 1990). GSH is therefore kept in a reduced state at a relatively high concentration of approximately 5–10 mmol/l in the cells by glutathione reductase. We found that the expression of the GSH synthase was significantly elevated with silver, which may imply that silver ions call for an increase of GSH in the cell. In plants and fungi GSH is enzymatically synthesized in response to toxic metals and forms metal chelate complexes that are thought to protect the plant from the metals (Zenk 1996; Li et al. 1995). Studies of yeast and bacteria have established that their resistance to metals involves GSH sequestration (Rebbeor et al. 1998; Li et al. 1996).

The metabolism and detoxification of xenobiotics including metals comprise three main phases (Li et al. 1996). Phase I is a preparatory step in which the toxins are oxidized, reduced, or hydrolysed to introduce or expose functional groups. Examples of phase I enzymes are cytochrome P450 and various oxidases. In phase II, the active derivate is conjugated with GSH, glucuronic acid or glucose. In the case of

the GSH-dependent pathway, complexes of GSH and xenobiotics are formed by the gluthatione S-transferase enzyme. In the final phase III of the GSH-dependent pathway, the complexes are eliminated from the cytosol by the GS-X pump (Li et al. 1996; Deeley et al. 2006). The GS-X pump is a member of the ATP binding cassette (ABC) protein superfamily, which transports a variety of substances across biological membranes, including drugs, peptides and toxic metals (Deeley et al. 2006). An example is the yeast cadmium factor (YCF1) gene required for cadmium resistance. This factor encodes an amino acid protein with extensive homology to the human multidrug resistance-associated protein (MRP1) (Li et al. 1996). The MRP1 isoform is often up regulated in cancer drug-treated cells since these cells are occupied with detoxification and efflux pumping of these xenobiotics (Ishikawa et al. 1994). Studies also provide evidence that the MRP1/GS-X pump is involved in transporting toxic metal complexes as GS-metals. For example, GS-cisplatin (a cancer drug containing platin), GS-arsenic and GS-cadmium are pumped by the MRP1 protein (Leslie et al. 2004; Li et al. 1996). Furthermore, there is a coordinated induction of the MRP/GS-X pump and GSH-synthase by heavy metals in human leukaemia cells (Ishikawa et al. 1996). MRP1 is present in a perinuclear region positive for lysomal markers (Rajagopal and Simon 2003) and the GST enzyme is also present in a microsomal fraction (Leslie et al. 2004). Thus, it is tempting to think that an MRP/GS-X pump is involved in pumping the silver-GS complexes into storage vesicles. This would explain our ultrastructural finding of silver–sulphur nanocrystals in lysosome-like vesicles. Our studies on the time-course mRNA expression profiles for a number of MRP isoforms revealed that the MRP2 isoform is upregulated by silver (Fig. 6). Thus, it is possible that the MRP2 isoform is involved in pumping GSH-silver complexes into the vesicles. Based on a multitude of studies we believe that the silver accumulation vesicles are lysosomes (also see Danscher and Stoltenberg 2006).

In conclusion, based on the present data we suggest that silver ions are sequestered partly by cellular uptake and partly by being attached to different kinds of collagen fibres. It seems as if the known cytotoxic effects of silver ions involves only the very surface of the wound and that detoxification processes restrain the toxic effects of the metal in the first few tens of microns into the undamaged tissue. We suggest that glutathione is a candidate of a dynamic molecular defence mechanism resulting in GSH-silver complexes being pumped into lysosomes.

Reference

Aaseth J, Olsen A, Halse J, Hovig T (1981) Argyria-tissue deposition of silver as selenide. Scand J Clin Lab Invest 41:247–251

Almar MM, Dierickx PJ (1990) In vitro interaction of mercury, copper (II) and cadmium with human glutathione transferase pi. Res Commun Chem Pathol Pharmacol 69:99–102

Bicanova M, Thinschmidt G (1985) Oligodynamic action of silver ions on micro-organisms. Pharmazie 40:736

Brett DW (2006) A discussion of silver as an antimicrobial agent: alleviating the confusion. Ostomy Wound Manage 52:34–41

Burd A, Kwok CH, Hung SC, Chan HS, Gu H, Lam WK, Huang L (2007) A comparative study of the cytotoxicity of silver-based dressings in monolayer cell, tissue explant, and animal models. Wound Repair Regen 15:94–104

Cole SP, Deeley RG (2006) Transport of glutathione and glutathione conjugates by MRP1. Trends Pharmacol Sci 27:438–446

Danscher G (1981) Light and electron microscopic localization of silver in biological tissue. Histochemistry 71:177–186

Danscher G, Stoltenberg M (2006) Silver enhancement of quantum dots resulting from (1) metabolism of toxic metals in animals and humans (2) in vivo, in vitro and immersion created zinc-sulphur/zinc-selenium nanocrystals, (3) metal ions liberated from metal implants and particles. Prog Histochem Cytochem 41:57–139

Deeley RG, Westlake C, Cole SP (2006) Transmembrane transport of endo- and xenobiotics by mammalian ATP-binding cassette multidrug resistance proteins. Physiol Rev 86:849–899

Hollinger MA (1996) Toxicological aspects of topical silver pharmaceuticals. Crit Rev Toxicol 26:255–260

Ishikawa T, Ali-Osman F (1993) Glutathione-associated cis-diamminedichloroplatinum(II) metabolism and ATP-dependent efflux from leukemia cells. Molecular characterization of glutathione-platinum complex and its biological significance. J Biol Chem 268:20116–20125

Ishikawa T, Bao JJ, Yamane Y, Akimaru K, Frindrich K, Wright CD, Kuo MT (1996) Coordinated induction of MRP/GS-X pump and gamma-glutamylcysteine synthetase by heavy metals in human leukemia cells. J Biol Chem 271:14981–14988

Ishikawa T, Wright CD, Ishizuka H (1994) GS-X pump is functionally overexpressed in cis-diamminedichloroplatinum (II)-resistant human leukemia HL-60 cells and down-regulated by cell differentiation. J Biol Chem 269:29085–29093

Jansson K, Kratz G, Haegerstrand A (1996) Characterization of a new in vitro model for studies of reepithelialization in human partial thickness wounds. In Vitro Cell Dev Biol Anim 32:534–540

Jorgensen B, Price P, Andersen KE, Gottrup F, Bech-Thomsen N, Scanlon E, Kirsner R, Rheinen H, Roed-Petersen J, Romanelli M, Jemec G, Leaper DJ, Neumann MH, Veraart J, Coerper S, Agerslev RH, Bendz SH, Larsen JR, Sibbald RG (2005) The silver-releasing foam dressing, contreet foam, promotes faster healing of critically colonised venous leg ulcers: a randomised, controlled trial. Int Wound J 2:64–73

Lansdown AB (2002) Metallothioneins: potential therapeutic aids for wound healing in the skin. Wound Repair Regen 10:130–132

Lansdown AB (2006) Silver in health care: antimicrobial effects and safety in use. Curr Probl Dermatol 33:17–34:17–34

Lansdown AB (2007) Critical observations on the neurotoxicity of silver. Crit Rev Toxicol 37:237–250

Lansdown AB, Sampson B, Laupattarakasem P, Vuttivirojana A (1997) Silver aids healing in the sterile skin wound: experimental studies in the laboratory rat. Br J Dermatol 137:728–735

Lansdown AB, Sampson B, Rowe A (1999) Sequential changes in trace metal, metallothionein and calmodulin concentrations in healing skin wounds. J Anat 195:375–386

Lansdown AB, Sampson B, Rowe A (2001) Experimental observations in the rat on the influence of cadmium on skin wound repair. Int J Exp Pathol 82:35–41

Lansdown AB, Williams A (2004) How safe is silver in wound care? J Wound Care 13:131–136

Lansdown AB, Williams A, Chandler S, Benfield S (2005) Silver absorption and antibacterial efficacy of silver dressings. J Wound Care 14:155–160

Leslie EM, Haimeur A, Waalkes MP (2004) Arsenic transport by the human multidrug resistance protein 1 (MRP1/ABCC1). Evidence that a tri-glutathione conjugate is required. J Biol Chem 279:32700–32708

Li ZS, Szczypka M, Lu YP, Thiele DJ, Rea PA (1996) The yeast cadmium factor protein (YCF1) is a vacuolar glutathione S-conjugate pump. J Biol Chem 271:6509–6517

Li ZS, Zhao Y, Rea PA (1995) Magnesium adenosine 5[prime]-triphosphate-energized transport of glutathione-S-conjugates by plant vacuolar membrane vesicles. Plant Physiol 107:1257–1268

Rajagopal A, Simon SM (2003) Subcellular localization and activity of multidrug resistance proteins. Mol Biol Cell 14:3389–3399

Ralat LA, Colman RF (2004) Glutathione S-transferase pi has at least three distinguishable xenobiotic substrate sites close to its glutathione-binding site. J Biol Chem 279:50204–50213

Rebbeor JF, Connolly GC, Dumont ME, Ballatori N (1998) ATP-dependent transport of reduced glutathione on YCF1, the yeast orthologue of mammalian multidrug resistance associated proteins. J Biol Chem 273:33449–33454

Rungby J, Danscher G (1984) Hypoactivity in silver exposed mice. Acta Pharmacol Toxicol (Copenh) 55:398–401

Scheuhammer AM, Cherian MG (1986) Quantification of metallothioneins by a silver-saturation method. Toxicol Appl Pharmacol 82:417–425

Shevchenko A, Wilm M, Vorm O, Mann M (2004) Mass spectrometric sequencing of proteins from silver-stained polyacrylamide gels. Anal Chem 68:850–858

Stoltenberg M, Danscher G (2000) Histochemical differentiation of autometallographically traceable metals (Au, Ag, Hg, Bi, Zn): protocols for chemical removal of separate autometallographic metal clusters in epon sections. Histochem J 32:645–652

Terrier P, Townsend AJ, Coindre JM, Triche TJ, Cowan KH (1990) An immunohistochemical study of pi class glutathione S-transferase expression in normal human tissue. Am J Pathol 137:845–853

Whalen R, Kempner ES, Boyer TD (1996) Structural studies of a human pi class glutathione S-transferase. Photoaffinity labeling of the active site and target size analysis. Biochem Pharmacol 52:281–288

Zenk MH (1996) Heavy metal detoxification in higher plants—a review. Gene 179:21–30